

# Early detection of T-cell lymphoma with T follicular helper phenotype by *RHOA* mutation analysis

Rachel Dobson,<sup>1</sup> Peter Y. Du,<sup>1</sup> Livia Rásó-Barnett,<sup>2</sup> Wen-Qing Yao,<sup>1</sup> Zi Chen,<sup>1</sup> Calogero Casa,<sup>2</sup> Hesham El-Daly,<sup>2</sup> Lorant Farkas,<sup>2,3</sup> Elizabeth Soilleux,<sup>1,4</sup> Penny Wright,<sup>4</sup> John W. Grant,<sup>4</sup> Manuel Rodriguez-Justo,<sup>5</sup> George A. Follows,<sup>6</sup> Hala Rashed,<sup>7</sup> Margarete Fabre,<sup>6,8</sup> E. Joanna Baxter,<sup>6</sup> George Vassiliou,<sup>6,8</sup> Andrew Wotherspoon,<sup>9</sup> Ayoma D. Attygalle,<sup>9</sup> Hongxiang Liu<sup>2</sup> and Ming-Qing Du<sup>1,4</sup>

<sup>1</sup>Division of Cellular and Molecular Pathology, Department of Pathology, University of Cambridge, Cambridge, UK; <sup>2</sup>The Haematopathology and Oncology Diagnostic Service, Addenbrooke's Hospital, Cambridge University Hospitals NHS Foundation Trust, Cambridge, UK; <sup>3</sup>Department of Pathology, Akershus University Hospital, Lorenskog, Norway; <sup>4</sup>Department of Histopathology, Addenbrooke's Hospital, Cambridge University Hospitals NHS Foundation Trust, Cambridge, UK; <sup>5</sup>Department of Pathology, Royal Free and University College Medical School, London, UK; <sup>6</sup>Department of Haematology, Addenbrooke's Hospital, Cambridge University Hospitals NHS Foundation Trust, Cambridge, UK; <sup>7</sup>Department of Cellular Pathology, University Hospitals of Leicester, East Midlands Pathology Services, Leicester, UK; <sup>8</sup>Wellcome-MRC Cambridge Stem Cell Institute, Jeffrey Cheah Biomedical Centre, University of Cambridge, Cambridge, UK and <sup>9</sup>Histopathology Department, The Royal Marsden Hospital, London, UK

## ABSTRACT

Angioimmunoblastic T-cell lymphoma (AITL) and peripheral T-cell lymphoma with T follicular helper phenotype (PTCL-TFH) are a group of complex clinicopathological entities that originate from T follicular helper cells and share a similar mutation profile. Their diagnosis is often a challenge, particularly at an early stage, because of a lack of specific histological and immunophenotypic features, paucity of neoplastic T cells and prominent polymorphous infiltrate. We investigated whether the lymphoma-associated *RHOA* Gly17Val (c.50G>T) mutation, occurring in 60% of cases, is present in the early “reactive” lesions, and whether mutation analysis could help to advance the early diagnosis of lymphoma. The *RHOA* mutation was detected by quantitative polymerase chain reaction with a locked nucleic acid probe specific to the mutation, and a further peptide nucleic acid clamp oligonucleotide to suppress the amplification of the wild-type allele. The quantitative polymerase chain reaction assay was highly sensitive and specific, detecting *RHOA* Gly17Val at an allele frequency of 0.03%, but not other changes in Gly17, nor in 61 controls. Among the 37 cases of AITL and PTCL-TFH investigated, *RHOA* Gly17Val was detected in 62.2% (23/37) of which 19 had multiple biopsies including preceding biopsies in ten and follow-up biopsies in 11 cases. *RHOA* Gly17Val was present in each of these preceding or follow-up biopsies including 18 specimens that showed no evidence of lymphoma by combined histological, immunophenotypic and clonality analyses. The mutation was seen in biopsies 0–26.5 months (mean 7.87 months) prior to the lymphoma diagnosis. Our results show that *RHOA* Gly17Val mutation analysis is valuable in the early detection of AITL and PTCL-TFH.

## Introduction

Angioimmunoblastic T-cell lymphoma (AITL), peripheral T-cell lymphoma with T follicular helper phenotype (PTCL-TFH) and follicular T-cell lymphoma are a group of complex clinicopathological entities that originate from T follicular helper (TFH) cells. These lymphomas are the most common among various T-cell malignancies in Western countries. Patients with these lymphomas commonly show an aggressive clinical course, with a median 3-year survival rate of only 30%



Haematologica 2022  
Volume 107(2):489-499

## Correspondence:

MING-QING DU  
mqd20@cam.ac.uk

Received: July 9, 2020.

Accepted: January 22, 2021.

Pre-published: February 11, 2021.

<https://doi.org/10.3324/haematol.2020.265991>

©2022 Ferrata Storti Foundation

Material published in *Haematologica* is covered by copyright. All rights are reserved to the Ferrata Storti Foundation. Use of published material is allowed under the following terms and conditions:

<https://creativecommons.org/licenses/by-nc/4.0/legalcode>.

Copies of published material are allowed for personal or internal use. Sharing published material for non-commercial purposes is subject to the following conditions:

<https://creativecommons.org/licenses/by-nc/4.0/legalcode>, sect. 3. Reproducing and sharing published material for commercial purposes is not allowed without permission in writing from the publisher.



(<https://www.hmrn.org/statistics/disorders/34>). The poor clinical outcome is largely a consequence of the lack of understanding of their molecular mechanism and targeted therapy.

The diagnosis of these lymphoma entities, particularly at an early stage, is a challenge because of the lack of specific clinical and histological features, low tumor cell content and the presence of prominent polymorphous inflammatory infiltrates that often mask the neoplastic cells. To help the diagnosis, T-cell clonality analysis is commonly used, but this is frequently not helpful because of the paucity of malignant T cells. The diagnostic difficulty is further exacerbated by the increasing use of needle core biopsies to avoid more invasive surgical excision. When a lymphoproliferative lesion is suspected but uncertain on histological diagnosis, patients are commonly subjected to a “watch and wait” approach, and further biopsied when showing signs of disease progression.

There is a wide range of genetic changes in T-cell lymphomas with TFH phenotype, including early *TET2* and *DNMT3A* mutations, which occur in hematopoietic stem cells, and late genetic changes, which are specifically seen in lymphoma cells.<sup>1-4</sup> Among the latter, *RHOA* mutation is the most frequent,<sup>2,5-9</sup> occurring in 60-70% of cases, with Gly17Val (c.50G>T) accounting for 95% of the changes. Interestingly, studies of mouse models have suggested that *RHOA* Gly17Val mutation induces TFH cell differentiation and, together with loss-of-function *TET2* mutations, can promote the development of AITL-like lymphomas.<sup>10-12</sup> Importantly, *RHOA* mutation is preferentially associated with the above lymphoma entities and has, so far, been shown only in the neoplastic T-cell population, but not in reactive B and T cells in these malignant conditions.<sup>2,5,13,14</sup> Studies to date suggest that the *RHOA* Gly17Val mutation could be used as a marker for the diagnosis of AITL and PTCL-TFH.<sup>6,15</sup> However, it is unclear whether the mutation is present in tissue biopsies prior to the diagnosis of AITL and whether mutation analysis could help in the early detection of these lymphomas. To investigate these issues, we established a highly sensitive quantitative polymerase chain reaction (qPCR) assay to detect the *RHOA* mutation, and screened a large cohort (n=37 cases) of AITL and PTCL-TFH with multiple sequential biopsies together with 61 controls.

## Methods

### Tissue materials and DNA extraction

The use of archival tissues for research was approved by the ethics committees of the institutions involved. In total, 78 tissue specimens from 37 patients (multiple consecutive specimens in 29 cases) with AITL (n=35) or PTCL-TFH (n=2), together with 61 controls (13 with reactive lymph nodes with paracortical expansion of T cells, 10 with classic Hodgkin lymphoma and 1 with marginal zone lymphoma with a prominent background of T cells) and peripheral blood DNA samples from 16 individuals (*TET2* and *DNMT3A* mutations in 2, *TET2* mutation in 4, *DNMT3A* mutation in 5) with clonal hematopoiesis of indeterminate potential (CHIP) (1 individual classed as having high-risk CHIP) were successfully investigated. DNA samples were prepared from a whole tissue section of each specimen. Purified DNA was obtained using a QIAamp DNA-Micro kit (Qiagen), while crude DNA was obtained by digesting samples at 37°C overnight with proteinase K and NP-40 buffer. Purified DNA samples from

nine cases of AITL or PTCL-TFH with known *RHOA* mutations (Gly17Val, c.50G>T, n=6 with variant allele frequency [VAF] ranging from 2-32%; Gly17Leu, c.49-50GG>TT, n=2; Gly17Glu, c.50G>A, n=1; Ser26Arg, c.76A>C, n=1) were available from our previous study,<sup>2</sup> while crude DNA samples were available from routine clonality analysis or similarly prepared. The histology of these specimens was reviewed by specialist hematopathologists.

### Quantitative polymerase chain reaction with peptide nucleic acid clamp and locked nucleic acid probe

The qPCR with peptide nucleic acid (PNA) clamp and locked nucleic acid (LNA) probe was performed as previously described.<sup>16</sup> The qPCR assay contained two probes and a PNA clamp (Figure 1A, *Online Supplementary Table S1*). The total probe served as an internal control to monitor the PCR performance. The PNA clamp specifically and strongly binds to the wild-type DNA sequence, resisting the 5' nuclease activity of Taq DNA polymerase, and thus blocks the wild-type allele from PCR amplification. This results in preferential amplification of the mutant allele which is detected specifically by the LNA mutant probe.

PCR primers with various probes were first tested using purified DNA samples, with the optimized conditions outlined below (*Online Supplementary Table S1*). Briefly, the PNA-LNA PCR was carried out in a 20 µL reaction containing 10 µL Premix Ex Taq (Probe qPCR) Master Mix (Takara, Shiga, Japan), 0.2 µM of each forward and reverse primer, 0.1 µM of each total and mutant probe, 0.05 µM of the PNA clamp probe, and 2 µL of crude DNA or 25 ng of purified DNA. Real-time PCR was carried out in triplicate using Quantstudio 6 (Thermo Fisher Scientific, Waltham, MA, USA) with denaturation at 95°C for 30 s followed by 45 cycles at 95°C for 3 s, and at 62°C for 30 s.

### Targeted sequencing using the Fluidigm Access Array and Illumina MiSeq

Targeted sequencing was performed on a selected case with consecutive tissue biopsies as described in our recent study.<sup>2</sup> Each of the DNA samples was investigated in duplicate for mutations in *TET2*, *DNMT3A*, *IDH2*, *RHOA*, *PLCG1*, *CCND3*, *CD28* and *TNFRSF21* by Fluidigm PCR and Illumina MiSeq sequencing. Sequence reads alignment, variant calling, filtering to eliminate false positive and benign changes were carried out according to our previously established protocols.<sup>2</sup> Only the reproducible variants that appeared in both replicates were regarded as true changes.

### BaseScope *in situ* hybridization

This was performed on a selected case. The sequence of the clonal TRB rearrangement in a case of AITL was available from a recent study.<sup>2</sup> Based on the unique VDJ junctional sequence, unique BaseScope probes were designed and used to identify the lymphoma T cells by *in situ* hybridization. The BaseScope *in situ* hybridization was carried out according to the manufacturer's instructions (Advanced Cell Diagnostics, Newark, CA, USA),<sup>2</sup> with the conditions optimized using the AITL specimen from which the clonal TRB rearrangement was sequenced. Tonsils were used as a negative control.

## Results

### Peptide nucleic acid - locked nucleic acid quantitative polymerase chain reaction is highly sensitive and specific for the detection of *RHOA* Gly17Val (c.50G>T)

Upon the optimization of PCR conditions for *RHOA* mutation detection, we first determined the sensitivity of

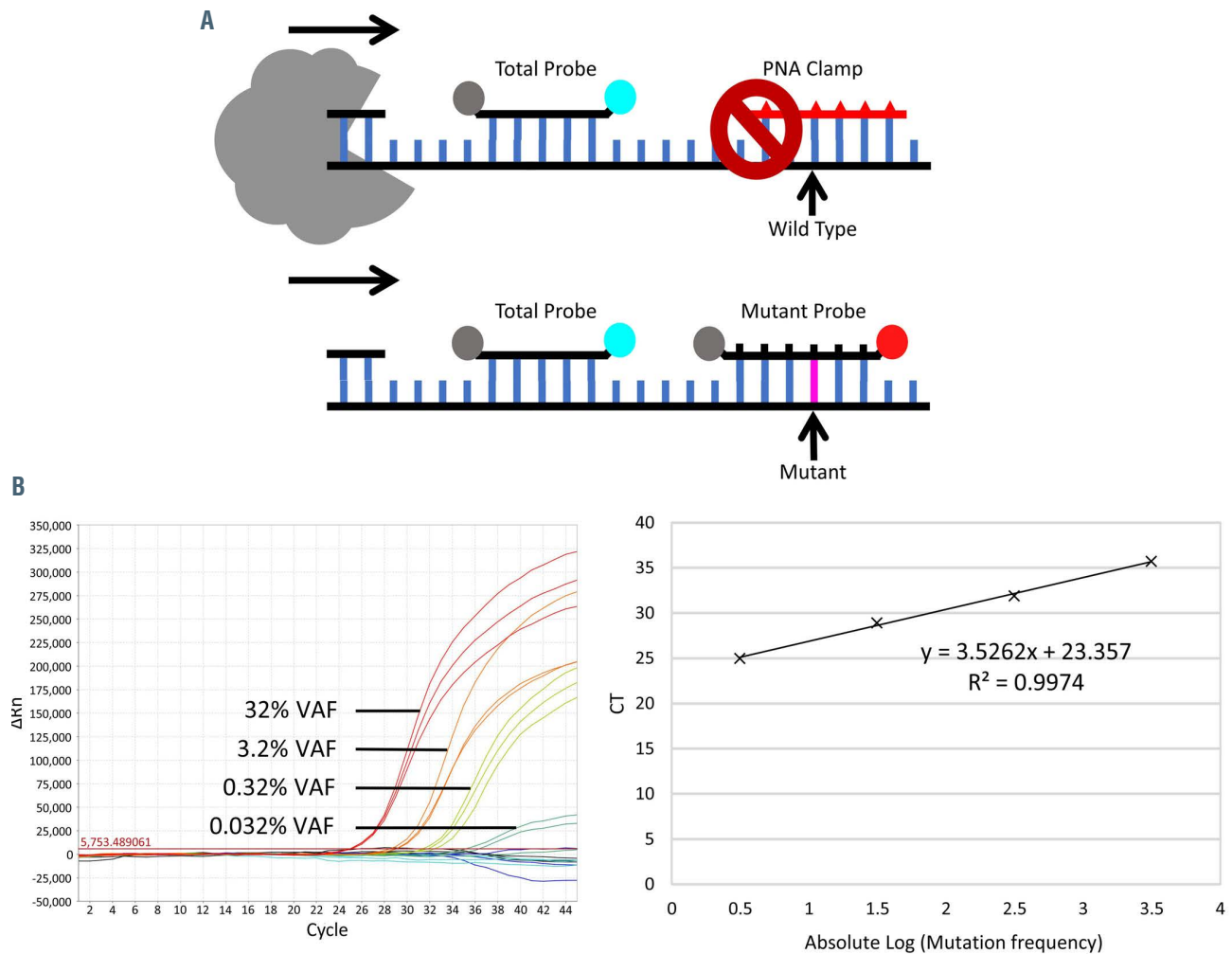


**Figure 1.** Detection of *RHOA* p.Gly17Val (c.50G>T) by real time polymerase chain reaction with peptide nucleic acid/locked nucleic acid probes. (A) Schematic illustration of the real time polymerase chain reaction (PCR) design. The total probe is used as an internal control to monitor the PCR performance. The peptide nucleic acid (PNA) clamp binds to the wild-type sequence, resists the 5' nuclease activity of Taq DNA polymerase and thus blocks the wild-type allele from PCR amplification. This results in preferential amplification of the mutant allele which is detected specifically by the locked nucleic acid (LNA) mutant probe. (B) The PCR assay is highly sensitive, capable of detecting the *RHOA* mutation at a variant allele frequency (VAF) of 0.03% based on serial dilutions of an angioimmunoblastic T-cell lymphoma sample with known mutation allele frequency by next-generation sequencing (left panel). For simplicity, only the LNA mutant but not total probe signals are shown. The PCR assay shows a linear correlation among the serial dilutions (right panel).

the qPCR assay using serial dilutions of three purified DNA samples with known VAF of Gly17Val (c.50G>T) into tonsil DNA. The PNA-LNA qPCR was highly sensitive, capable of detecting the mutation at a VAF of 0.032% (Figure 1B). As expected, the qPCR was highly specific to Gly17Val (c.50G>T) and showed no detectable signal of the LNA mutant probe with the DNA samples harboring other *RHOA* mutations including Gly17Leu (c.49-50GG>TT) and Gly17Glu (c.50G>A), or tonsillar DNA (Online Supplementary Figure S1A).

As crude DNA preparations were routinely used for clonality analysis in our clinical diagnostic laboratories, we tested whether such crude DNA samples were amenable to the above PNA-LNA qPCR (Online Supplementary Figure S1C). Of the ten crude DNA samples initially tested, nine yielded excellent amplification comparable with the results from purified DNA samples. We then used crude DNA preparations for the qPCR in the remaining investigations, with high quality results from 139 of the 144 samples investigated. The reason that the other five samples failed to support qPCR was

essentially the poor quality of the DNA, as evidenced by quality control PCR.

### ***RHOA* Gly17Val (c.50G>T) is detected in initial biopsies not diagnostic for lymphoma by conventional approaches**

To confirm that the *RHOA* mutation was lymphoma-specific, not associated with reactive conditions proliferations or other lymphoproliferative disorders with enriched T cells, we investigated 45 tissue biopsies including 27 from lymph nodes, for which T-cell clonality analysis was requested during routine histological diagnosis, but showed no evidence of a T-cell lymphoma. These included 13 specimens showing paracortical T-cell expansion or enriched CD4<sup>+</sup> T cells, and ten classic Hodgkin lymphomas with a prominent background of T cells. The qPCR was successful for all these specimens, as indicated by the total probe control, but they were all negative for the *RHOA* mutation. Similarly, we also showed absence of the *RHOA* mutation in peripheral blood lymphocytes (Online Supplementary Figure S1D)

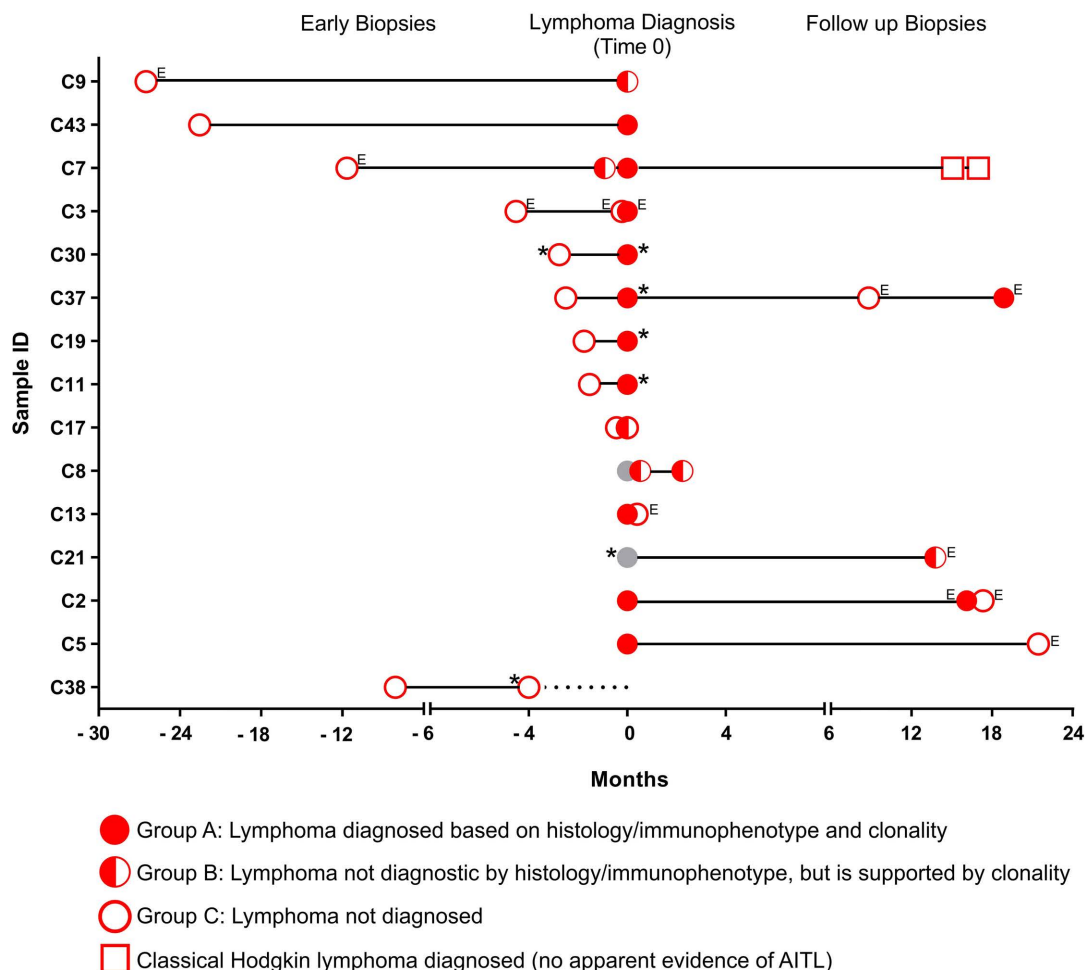


Figure 2. Analysis of *RHOA* (c.50G>T; p.Gly17Val) mutation by quantitative polymerase chain reaction in the *RHOA*-positive cases with longitudinal biopsies in patients with angioimmunoblastic T-cell lymphoma (only including cases with at least one biopsy classed as not diagnostic ["group B" or "group C"]). The diagnoses of these specimens were reviewed, and categorized into three groups: group A (filled circles): lymphoma diagnosed by histology and immunophenotype, further supported by clonal TCR gene rearrangement; group B (half-filled circles): lymphoma not diagnostic by histology and immunophenotype alone, but ascertained by clonal TCR gene rearrangement; group C (open circles): lymphoma not diagnosed by combined analyses. Red (regardless of the symbol: including outline only, half-filled, and completely filled symbols) indicates *RHOA* p.Gly17Val mutant positive biopsy. Gray indicates *RHOA* p.Gly17Val status unknown. E denotes extranodal biopsies. \*denotes lymph node excision biopsies and all others are core biopsy specimens. An open square denotes a diagnosis of classic Hodgkin lymphoma with no apparent evidence of angioimmunoblastic T-cell lymphoma (AITL). Case 38 lacks a final diagnosis as the patient died, indicated by a dashed line. Cases with only group A multiple biopsies are not included in this figure.

from 16 individuals with CHIP (mutational information provided in *Online Supplementary Table S2*), in keeping with the findings from whole exome or panel sequencing.<sup>17,18</sup>

We then investigated 37 cases of AITL (n=35) or nodal PTCL-TFH (n=2) with unknown *RHOA* mutation status, of which 29 had multiple longitudinal biopsies (2-5) available for *RHOA* analysis. *RHOA* mutation was seen in 23 cases, but was negative in the remaining 14 cases. Among the 23 cases with *RHOA* mutation, 19 cases had multiple biopsies. We reviewed the original histological diagnosis in each of these specimens and categorized them into three groups. Group A specimens (n=26) showed clear evidence of lymphoma by histology and immunophenotype, further supported by clonal TCR rearrangement. Group B (n=6) had suspicious histological and immunophenotypic findings, although not entirely diagnostic for lymphoma, which was ascertained by detection of strong clonal TCR gene rearrangements. Finally, group C mutations (n=18) were not diagnostic for lymphoma by combined histological, immunophenotypic

and clonality analyses (*Online Supplementary Table S3*). Interestingly, *RHOA* mutation was detected in each of these specimens, in the positive cases, including those not diagnostic for lymphoma by conventional integrated diagnostic investigations (Figure 2).

#### Characteristics of biopsies not diagnostic for lymphoma but positive for *RHOA* mutation

Of the 23 cases of AITL or PTCL-TFH with *RHOA* mutation, the initial biopsy was not diagnostic in ten cases including two with an excisional lymph node specimen. The time from the initial non-diagnostic biopsy to that establishing AITL or PTCL-TFH ranged from 0 to 26.5 months, with an average of 7.87 months. All these initial non-diagnostic biopsies showed polyclonal (n=4), weak clonal (n=5) or oligoclonal (n=2) TCR gene rearrangements or failed (n=1) by BIOMED-2 TRB and TRG clonality analysis. Seven of the initial non-diagnostic biopsies were also subjected to BIOMED-2 B-cell clonality analysis and six showed a clonal *IG* gene rearrangement. Epstein-Barr virus (EBV)-encoded small RNA

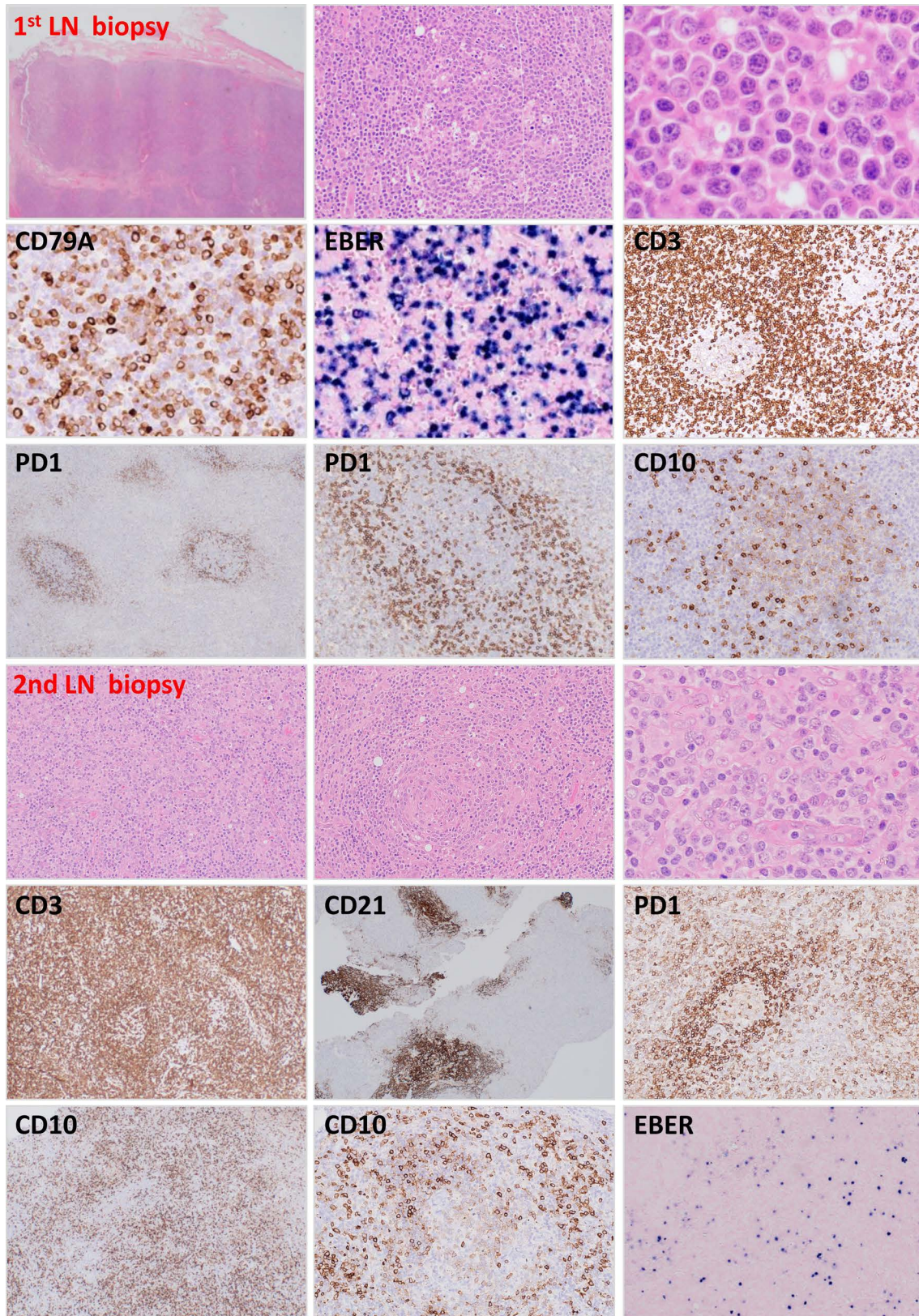


Figure 3. Histological and immunophenotypic findings in case 30. The first lymph node excision biopsy shows partial effacement of the lymph node architecture by polymorphous infiltrates, particularly B cells with plasmacytoid differentiation. A large proportion of B cells were EBER-positive and showed Ig  $\kappa$  light chain restriction (not shown). The lymphoid follicles appear to be reactive and shows no apparent expansion of T follicular helper (TFH) cells, with only a few CD10-positive cells spilling out of the germinal center, consistent with pattern-1 histology of angioimmunoblastic T-cell lymphoma (AITL). The second lymph node biopsy shows effacement of the lymph node architecture by medium-sized atypical lymphoid cells with regressed follicles. There is a prominent proliferation of follicular dendritic cell meshworks and high endothelial venules with atypical lymphoid cells clustered in their vicinity. The atypical lymphoid cells are T cells expressing TFH markers, spilling out of the germinal center to the interfollicular region. EBER *in situ* hybridization shows only scattered positive cells.

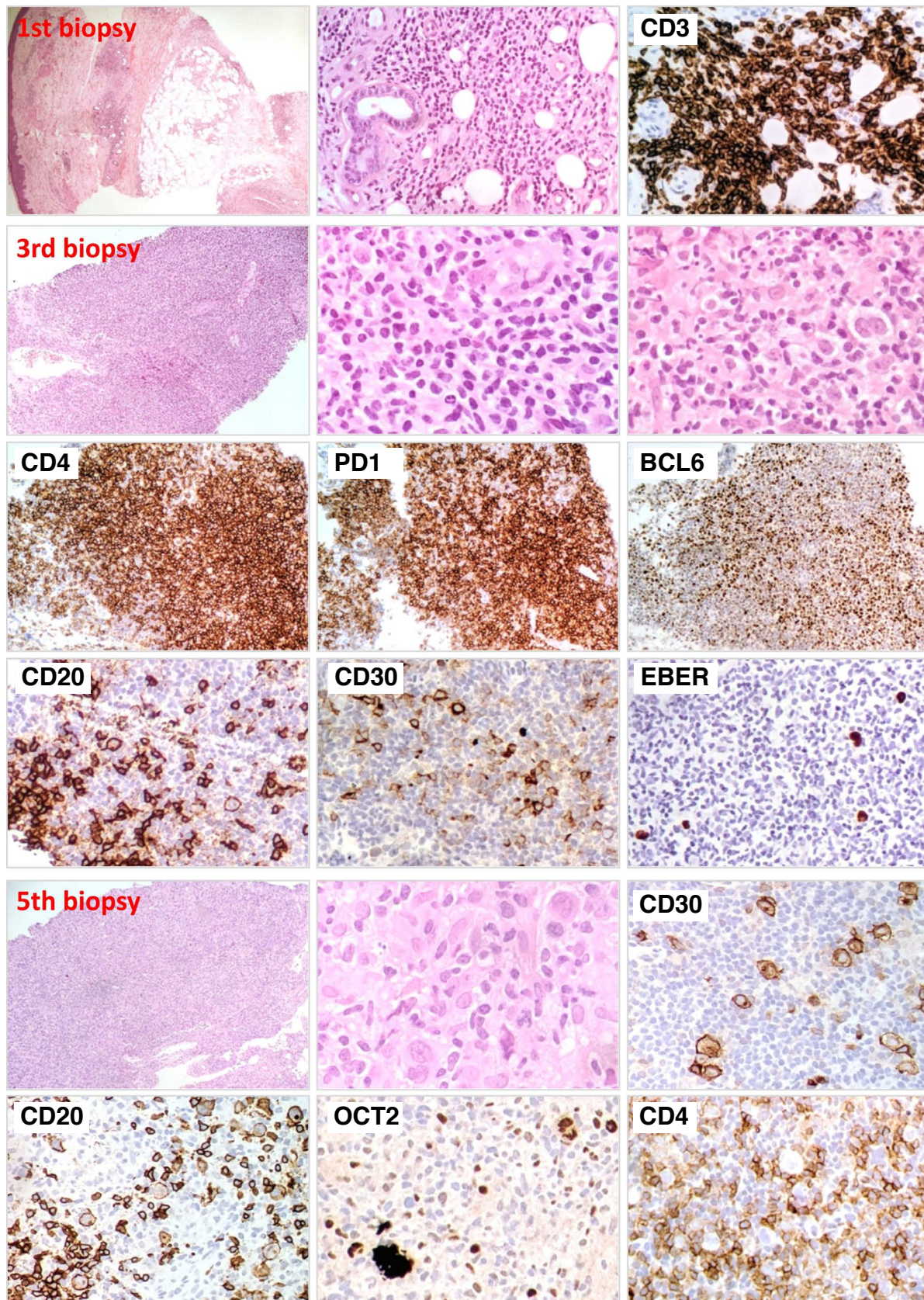


Figure 4. Histological and immunophenotypic findings in case 7. The first biopsy shows a subcutaneous perivascular infiltrate of CD3<sup>+</sup> T cells with vasculitic features. The third biopsy shows cardinal features of angioimmunoblastic T-cell lymphoma (AITL) and also a prominent pleomorphic infiltrate including an EBER-positive B-cell population with Hodgkin and Reed/Sternberg (HRS)-like morphology and immunophenotype. The fifth biopsy shows no apparent evidence of AITL, but a polymorphous infiltrate with a more prominent EBER-positive B-cell population that has HRS cell morphology and immunophenotype, rosetting by CD4<sup>+</sup> T cells.

**Table 1. Summary of histological, immunohistochemical, clonality analysis and genetic findings in case 7.**

	First biopsy	Second biopsy	Third biopsy	Fourth biopsy	Fifth biopsy
Time after the 1 <sup>st</sup> biopsy		11 months later	11.5 months later	33 months later	35 months later
Clinical presentation	Skin rash, fevers; All self-resolved with no therapy	Episode of non-specific symptoms; lymphadenopathy revealed by CT, but relatively low PET signal; opted for close surveillance.		Slowing enlarging lymph node with increasing symptoms. Treated with 6 cycles of R-GCVP* and achieved CR; Ongoing remission in May 2020	
Biopsy site	Skin punch biopsy	Lymph node core biopsy	Left axillary lymph node core biopsy	Right axillary lymph node core biopsy	Right axillary lymph node core biopsy
Histology and Immuno-phenotype	Mild perivascular infiltrate, predominantly CD3 <sup>+</sup> T cells, admixed histiocytes and B cells	Predominant infiltrate of small to medium sized T cells with vasocentric pattern, CD4 <sup>+</sup> , some CD10 <sup>+</sup> and BCL6 <sup>+</sup> T cells possibly spilled outside B-cell follicle, expanded FDC meshworks; scattered large EBER <sup>+</sup> B cells: CD30 <sup>+</sup> , CD15 weak <sup>+</sup>	Very similar to the 2nd biopsy. Predominantly small to medium sized T cells associated with HEV proliferation, CD4 <sup>+</sup> , PD1 <sup>+</sup> , BCL6 variable <sup>+</sup> ; Expanded FDC and pleomorphic infiltrate, scattered large B cells with HRS morphology CD30 <sup>+</sup> , CD15 weak <sup>+</sup>	Lymph node structure effaced by polymorphous infiltrate with scattered large atypical cells expressing CD30, CD20 (weak), CD79, PAX5, BCL6, MUM1, OCT2, BOB1, and EBER <sup>+</sup> , but not CD15. CD3 T cells: largely CD4 <sup>+</sup> , some ICOS <sup>+</sup> , occasional PD1 <sup>+</sup> , but CD10 <sup>-</sup> and CXCL13 <sup>-</sup>	Normal structure largely effaced by polymorphous infiltrate with prominent large atypical cells expressing CD30, CD20, CD79a, PAX5, MUM1, BCL6(weak), and EBER <sup>+</sup> , but not CD15, CD10, CYCLIN D1, ALK and CD25. No detectable T-cell abnormalities
Diagnosis	Panniculitis	AITL	AITL lymphoma	Classic Hodgkin lymphoma	Classic Hodgkin
T-cell clonality					
TRG-A	n/a	217 bp	217 bp	Poly	Poly
TRG-B	n/a	Poly	Poly	Poly	Poly
TRB-A	n/a	245 bp	245 bp	Poly	Poly
TRB-B	n/a	Poly	Poly	Poly	Poly
TRB-C	n/a	302 bp	Poly	Poly	187bp
B-cell clonality	n/a	n/a	n/a	Poly	Poly
BaseScope-ISH for TRB-V5-	Few positive cells	Diffuse positive	Diffuse positive	n/a	Negative
Targeted sequencing	n/a	<i>DNMT3A</i> (VAF: 34%) (c.920C>T; p.P307L) <i>TET2</i> (VAF: 8%) (c.3646C>T; p.R1216X) <i>TET2</i> (VAF: 36%) (c.3781C>A; p.R1261S) <i>TET2</i> (VAF: 3%) (c.3866G>T; p.C1289F) <i>TET2</i> (VAF: 18%) (c.4947T>A; p.Y1649X) <i>RHOA</i> (VAF: 20%) (c.50G>T; p.G17V)	n/a	n/a	<i>DNMT3A</i> (VAF:20%) (c.920C>T; p.P307L) <i>TET2</i> (VAF: 4%) (c.3646C>T; p.R1216X) <i>TET2</i> (VAF: 20%) (c.3781C>A, p.R1261S) <i>TET2</i> (VAF: 8%) (c.3866G>T; p.C1289F) <i>RHOA</i> (VAF: 1%) (c.50G>T; p.G17V)
<b>RHOA c.50G&gt;T</b>	Weak positive	Strong positive	Strong positive	Weak positive	Weak positive

n/a: not available; R-GCVD: rituximab, gemcitabine, cyclophosphamide, vincristine, prednisolone; CR: complete remission; VAF: variant allele frequency.

(EBER) *in situ* hybridization was carried out in eight cases during the routine diagnostic workup, and four showed variable positivity from a few scattered to numerous EBER-positive cells, of which three displayed clonal IG gene rearrangement. In four cases, EBV-driven proliferation or classic Hodgkin lymphoma were considered in the initial diagnosis.

Six follow-up biopsies were not diagnostic of involvement by AITL or PTCL-TFH by routine diagnostic investigations; these included two bone marrow and two skin specimens. In each specimen, a CD4<sup>+</sup> T-cell infiltrate was noted, but a definite aberrant immunophenotype and expression of TFH markers could not be ascertained. T-cell clonality analysis showed weak polyclonality in two and a weak clonal or oligoclonal pattern in two.

### Representative cases

**Case 30.** A 79-year-old man presented with bilateral tender neck lymph nodes, and had mild sweats, but no weight loss or fever. Clinical examination revealed multiple bilaterally enlarged neck and groin lymph nodes (up to 1.5 cm diameter), and palpable liver and spleen. Right level II neck lymph node excision biopsy showed partial effacement of the lymph node architecture and expansion of the interfollicular area by a polymorphous population of lymphoid cells, including B cells with plasmacytoid differentiation, and scattered large cells (Figure 3). These B cells expressed pan B-cell markers (CD20, CD79a, CD19), and MUM1, but were negative for CD10 and BCL6 (*data not shown*). A high proportion of the B cells were EBER-positive and showed IG  $\kappa$  light chain restriction. The lymphoid follicles appeared to be reactive and showed no apparent expansion of TFH cells, with only a few CD10-positive cells spilling out of the germinal centers (Figure 3). BIOMED-2 clonality analyses showed clonal IGH and IGK gene rearrangements, but a weak oligoclonal pattern with TRG and TRB. The histological diagnosis was uncertain: a clonal EBV-positive polymorphous lymphoproliferation was considered. Close follow-up with a low threshold for re-biopsy was recommended.

Two months later, the patient presented with increasing fatigue, fever, maculopapular chest rash and increased size of peripheral lymphadenopathy. Positron-emission tomography (PET) scan revealed extensive bilateral cervical, mediastinal, bilateral iliac and groin lymphadenopathy. Left level V neck lymph node excision biopsy showed partial effacement of the lymph node architecture by an infiltrate of medium-sized atypical lymphoid cells with regressed follicles (Figure 3). There was hyperplasia of follicular dendritic cell meshworks and high endothelial venules with the atypical lymphoid cells clustered in their vicinity. The atypical lymphoid cells were positive for CD3, CD5 and TFH markers (PD1, CD10, ICOS, BCL6) (Figure 3). EBER *in situ* hybridization revealed only scattered positive cells. BIOMED-2 clonality analyses showed clonal TRB and TRG gene rearrangements, and also weak clonal IGH and IGK gene rearrangements which were different from those of the previous biopsy in the size of their amplified IG products. A diagnosis of AITL was made. The patient was initially treated with six cycles of CHOP (cyclophosphamide, doxorubicin, vincristine, and prednisone), then avelumab (cycle 12 at the most recent follow-up) under the AVAIL-T trial, and was well, showing no constitutional symptoms or palpable cervical lymph nodes, 20 months following the AITL diagnosis.

Retrospective analysis showed the presence of *RHOA* Gly17Val mutation in the above two specimens by qPCR and targeted sequencing with 3% and 23% VAF in the first and second biopsy, respectively. The targeted sequencing also revealed a pathogenic nonsense substitution in *DNMT3A* (c.2311C>T, p.R771\*) in the first and second biopsy with 17% and 26% VAF, respectively.

**Case 7.** An 82-year-old man, with remission of a previous mantle cell lymphoma, presented with a skin rash on the right calf. A punch biopsy showed a mild perivascular infiltrate by CD3<sup>+</sup> T cells, with a histological diagnosis of panniculitis (Figure 4, Table 1). To investigate potential lymphoma relapse, lymph node core biopsies were taken at 11 and 12 months of follow-up: neither specimen showed evidence of mantle cell lymphoma, but both revealed cardinal features of AITL and also a prominent pleomorphic infiltrate including an EBER-positive B-cell population with Hodgkin and Reed/Sternberg (HRS)-like morphology and immunophenotype (Figure 4, Table 1). T-cell clonality analysis demonstrated clonal rearrangements by TRG-A and TRB-A with identical sized amplified products between the two biopsies, and an additional clonal rearrangement by TRB-C in the second biopsy. Further follow-up biopsies were taken at 25 and 26 months, and neither showed apparent evidence of AITL, but both had polymorphous infiltrates with a more prominent EBER-positive B-cell population that had HRS-cell morphology and immunophenotype (Figure 4, Table 1). Neither specimen showed any evidence of the clonal TRG/TRB rearrangements seen in the early lymph node biopsies, although a fifth biopsy displayed an isolated clonal rearrangement by TRB-C. B-cell clonality analyses demonstrated polyclonal IG gene rearrangements in both specimens (Figure 4, Table 1). A classic Hodgkin lymphoma arising from the EBV-positive B-cell component of the AITL was considered.

In a retrospective study, the TRB-A and B PCR products from the second biopsy were sequenced using an Illumina MiSeq platform and a dominant TRBV5-J2 rearrangement (86%) was identified.<sup>2</sup> Based on the unique VDJ junctional sequence, we designed unique BaseScope probes to identify the lymphoma T cells by *in situ* hybridization (*Online Supplementary Figure S2*). As expected, both the second and third biopsies with an AITL diagnosis showed diffuse positivity with the lymphoma clone-specific probe. Interestingly, the initial skin biopsy also displayed isolated positive cells, while the fifth biopsy with a diagnosis of EBV lymphoproliferative disease (LPD) gave a negative result. Both the second (AITL) and fifth (EBV-LPD) biopsies were investigated by panel sequencing for recurrent somatic mutations, and this identified five shared mutations – one *DNMT3A*, three *TET2* and one *RHOA* changes – between the two specimens, and one further *TET2* mutation only in the second specimen (Table 1). In general, the mutation load in each of the above shared changes was much higher in the second biopsy (AITL) than in the fifth biopsy (EBV-LPD). This was particularly striking for the *RHOA* Gly17Val mutation, with a VAF of 20% in the second biopsy but of only 1% in the fifth biopsy. As expected, qPCR for the *RHOA* mutation demonstrated its strong positivity in both the second and third biopsies showing AITL, but a weak positive signal in the initial skin biopsy, and the fourth and fifth biopsies displaying classic Hodgkin lymphoma-like EBV-LPD (Figure 4, *Online Supplementary Figure S2*).

## Discussion

By using a highly sensitive qPCR assay, we confirmed that *RHOA* Gly17Val (c.50G>T) mutation is specifically associated with AITL or PTCL-TFH, but is not found in other lymphoproliferative conditions including those with florid infiltration of T-helper cells. More importantly, detection of *RHOA* Gly17Val (c.50G>T) mutation could help early detection of AITL and PTCL-TFH, and also diagnosis of their extranodal involvement.

The difficulty in making a histological diagnosis of AITL or PTCL-TFH is well recognized, particularly when the neoplastic cell content is low, inconspicuous by histological and immunophenotypic assessment and undetectable by analysis of TCR gene rearrangements. Apart from the paucity of neoplastic T cells, the polymorphous infiltrate, particularly the presence of numerous EBV-positive B cells, including HRS-like cells (EBV-positive or -negative), may lead to diagnostic consideration of an EBV-driven B-cell proliferation.<sup>19-21</sup> Such misleading diagnostic features may also be reinforced by the frequent demonstration of clonal IG gene rearrangement. As shown in this study, EBV-driven B-cell proliferation was considered as a diagnosis in four of 11 of the initial biopsies. Indeed, it has been reported by several independent studies that EBV-associated lymphoproliferation is a frequent pitfall in the diagnosis of AITL.<sup>19-22</sup>

In the present study, the majority of the initial specimens that were not diagnostic were core biopsies. It is possible that these core biopsies were not totally representative, with characteristic lymphoma components missed because of sampling errors. Nevertheless, two initial non-diagnostic biopsies were excisional lymph node specimens, indicating that an absence of diagnostic features of AITL/PTCL-TFH in the initial biopsies was also a real issue. Interestingly, the time interval between the initial non-diagnostic biopsies and the follow-up biopsies that established the diagnosis varied considerably, ranging from 0 to 26.5 months. In the cases with a long interval, it is likely that the initial biopsy represented an early pre-malignant lesion, while the follow-up biopsy reflected more progressed disease, thus having more cardinal features for making the AITL/PTCL-TFH diagnosis. While in the cases with a short interval, it is possible that the enlarged lymph nodes were variably involved by AITL/PTCL-TFH and the initial non-diagnostic biopsies represented early involvement by the lymphoma.

Both the above possibilities may exist, without excluding the other. It is impossible to distinguish the two scenarios based on the analysis of a single biopsy, including *RHOA* mutation analysis. Nonetheless, detection of *RHOA* Gly17Val (c.50G>T) mutation can certainly raise the alarm to perform more in-depth histological and immunophenotypic investigations, for example a more careful search for evidence of TFH cell expansion, as shown in the first biopsy in case 30. It is important to emphasize that detection of a *RHOA* mutation is not equivalent to a diagnosis of lymphoma because mutational analysis by qPCR or targeted sequencing is highly sensitive, and the mutation is seen in biopsies without histological evidence of AITL. As discussed above, the *RHOA* mutation-positive non-diagnostic biopsy may represent a premalignant lesion or early involvement by the lymphoma. Therefore, *RHOA* mutation analysis should be used as an auxiliary tool with the results interpreted in the

context of histological and immunophenotypic findings. If a histological diagnosis of AITL/PTCL-TFH cannot be made, an excision biopsy or a low threshold for an early follow up biopsy, when appropriate, is indicated.

In a few case studies, *RHOA* mutation was detected in circulating free DNA or peripheral blood lymphocytes from patients with AITL/PTCL-TFH,<sup>15</sup> and the mutation burden appeared to correlate with the treatment outcome.<sup>23,24</sup> It remains to be investigated whether the mutation is detectable in circulating free DNA or peripheral blood lymphocytes at the time of initial non-diagnostic biopsies. Given that the *RHOA* mutation burden in circulating free DNA and peripheral blood lymphocytes reflects, at least theoretically, the overall lymphoma load, simultaneously analyzing blood samples, in addition to tissue biopsy, could add further value in lymphoma diagnosis, particularly when a specimen is not representative.

Apart from the initial biopsies, the diagnosis of extranodal involvement by AITL/PTCL-TFH such as skin and bone marrow is also difficult for reasons similar to those discussed above, including low tumor cell content and polymorphous infiltrate.<sup>25</sup> In particular, extranodal infiltrates may not harbor the cardinal features of AITL such as TFH marker expression in the neoplastic T cells and follicular dendritic cell meshworks. The DNA sample from these extranodal sites is often not informative for clonality analysis because of insufficient lymphoid cells and/or poor DNA quality. As shown in our study, *RHOA* mutation analysis is highly valuable for confirming AITL/PTCL-TFH involvement in follow-up biopsies. Similarly, *RHOA* mutation analysis is valuable in the diagnosis of AITL/PTCL-TFH from cytological specimens.<sup>9</sup>

Aside from the *RHOA* mutation, there are several other genetic changes including *IDH2*, *CD28*, *PLCG1*, *VAV1* and *TNFRSF21* mutations, and *VAV1-*STAP2**, *CTLA4-*CD28** and *ITK-SYK* fusions, which occur at variable frequencies in AITL and PTCL-TFH.<sup>2,26-28</sup> Of note, mutations in *VAV1*, a signaling molecule downstream of TCR, occurs in 8.2% of AITL and appears to be mutually exclusive of the *RHOA* mutation.<sup>28</sup> Detection of these additional lymphoma-associated genetic changes could also help the early detection of AITL/PTCL-TFH, together with *RHOA* mutation detection, potentially being valuable for diagnosis in up to 90% of these T-cell lymphomas. These diverse genetic changes could be readily investigated by targeted sequencing either alone or as part of a comprehensive lymphoma panel.

The detailed analyses of multiple biopsies in case 7 also revealed the mutation burden in non-malignant T cells. The fifth lymph node biopsy showed little involvement by AITL as the lymphoma clone was undetectable by BaseScope *in situ* hybridization and the VAF of the *RHOA* mutation was only 1%, but the specimen had a high *TET2* mutation burden (20% VAF). This implies that the *TET2* mutation must have been present in a large proportion of reactive B and T cells,<sup>1,5,29-31</sup> probably up to 40% of the total cell population, which is well above the EBER-positive cell fraction (~5%). Hence, this enlarged lymph node was essentially caused by lymphoid proliferation driven by the *TET2* mutation and/or EBV infection. These findings further highlight the markedly variable histological presentation of enlarged lymph nodes in patients with AITL and, hence, the danger of potential sampling errors in the diagnosis of AITL. In this context, it is pertinent to

investigate *RHOA* and other lymphoma-associated mutations in patients with advanced age and biopsies showing EBV-positive polymorphous infiltrates, to explore how such mutation analyses can help to circumvent this diagnostic pitfall. At the genetic level, the high number of *TET2* mutations and their frequent presence in non-neoplastic T cells suggest that the patient most likely had an underlying CHIP with *TET2* and *DNMT3A* mutations that occurred in hematopoietic stem cells, consequently extending to the progenies of these cells.

In general, patients with AITL typically have an aggressive clinical course and respond poorly to currently available therapies. Case 7 appeared to be an exception to this rule, showing slow disease progression in the absence of any treatment, although it is not possible to rule out a response to the R-GCVP (rituximab, gemcitabine, cyclophosphamide, vincristine, prednisolone) that was aimed at treating the EBV-associated proliferations (Table 1). An indolent clinical course has been previously reported for some patients with AITL showing pattern-1 histology, including those treated only with steroids.<sup>22,32</sup> It remains to be investigated how to identify such indolent cases at the time of diagnosis and stratify their clinical management accordingly, particularly in view of the advance in early detection of AITL.

In summary, we have shown that *RHOA* mutation is specifically associated with AITL, PTCL-TFH and their related lesions, and investigation of the mutation is highly valuable in early detection of these T-cell lymphomas and their extranodal involvement.

## Disclosures

No conflicts of interest to disclose.

## Contributions

RD, PD, WQ, and CC designed the experiments and collected and analyzed data; WQ and ZC performed the Illumina sequencing analysis and variant calling; LRB, HED, LF, ES, PW, JWG, MRJ, GAF, HR, AW, ADA, HL, MF, EJB, and GV contributed cases and pathology review; MQD and RD wrote and prepared the manuscript; MQD was responsible for research funding, study design and coordination. All authors commented on the manuscript and approved its submission for publication.

## Acknowledgments

The authors thank Shubha Anand and Yuanxue Huang for their assistance with using TapeStation, Graeme Clark and Ezequiel Martin for their assistance with Illumina sequencing and Fangtian Wu for carrying out DNA extraction on a control case.

## Funding

The research in MQD's laboratory was supported by grants from Blood Cancer UK (13006, 15019), CRUK (C8333/A29707), and the Kay Kendall Leukaemia Fund (KKL582) UK. WY was supported by a research fellowship from the China Scholarship Council, and an International Collaborative Award from the Pathological Society of Great Britain and Ireland, UK. The Human Research Tissue Bank is supported by the NIHR Cambridge Biomedical Research Centre.

## References

- Nguyen TB, Sakata-Yanagimoto M, Asabe Y, et al. Identification of cell-type-specific mutations in nodal T-cell lymphomas. *Blood Cancer J*. 2017;7(1):e516.
- Yao WQ, Wu F, Zhang W, et al. Angioimmunoblastic T-cell lymphoma contains multiple clonal T-cell populations derived from a common *TET2* mutant progenitor cell. *J Pathol*. 2020;250(3):346-357.
- Iqbal J, Amador C, McKeithan TW, Chan WC. Molecular and genomic landscape of peripheral T-cell lymphoma. *Cancer Treat Res*. 2019;176:31-68.
- Xie M, Lu C, Wang J, et al. Age-related mutations associated with clonal hematopoietic expansion and malignancies. *Nat Med*. 2014;20(12):1472-1478.
- Sakata-Yanagimoto M, Enami T, Yoshida K, et al. Somatic *RHOA* mutation in angioimmunoblastic T cell lymphoma. *Nat Genet*. 2014;46(2):171-175.
- Nakamoto-Matsubara R, Sakata-Yanagimoto M, Enami T, et al. Detection of the G17V *RHOA* mutation in angioimmunoblastic T-cell lymphoma and related lymphomas using quantitative allele-specific PCR. *PLoS One*. 2014;9(10):e109714.
- Palomero T, Couronne L, Khiabani H, et al. Recurrent mutations in epigenetic regulators, *RHOA* and *FYN* kinase in peripheral T cell lymphomas. *Nat Genet*. 2014;46(2):166-170.
- Ondrejka SL, Grzywacz B, Bodo J, et al. Angioimmunoblastic T-cell lymphomas with the *RHOA* p.Gly17Val mutation have classic clinical and pathologic features. *Am J Surg Pathol*. 2016;40(3):335-341.
- Lee PH, Weng SW, Liu TT, et al. *RHOA* G17V mutation in angioimmunoblastic T-cell lymphoma: a potential biomarker for cytological assessment. *Exp Mol Pathol*. 2019;110:104294.
- Zang S, Li J, Yang H, et al. Mutations in 5-methylcytosine oxidase *TET2* and *RhoA* cooperatively disrupt T cell homeostasis. *J Clin Invest*. 2017;127(8):2998-3012.
- Cortes JR, Ambesi-Impiombato A, Couronné L, et al. *RHOA* G17V induces T follicular helper cell specification and promotes lymphomagenesis. *Cancer Cell*. 2018;33(2):259-273.
- Ng SY, Brown L, Stevenson K, et al. *RhoA* G17V is sufficient to induce autoimmunity and promotes T-cell lymphomagenesis in mice. *Blood*. 2018;132(9):935-947.
- Dobay MP, Lemonnier F, Missaglia E, et al. Integrative clinicopathological and molecular analyses of angioimmunoblastic T-cell lymphoma and other nodal lymphomas of follicular helper T-cell origin. *Haematologica*. 2017;102(4):e148-e151.
- Yoo HY, Sung MK, Lee SH, et al. A recurrent inactivating mutation in *RHOA* GTPase in angioimmunoblastic T cell lymphoma. *Nat Genet*. 2014;46(4):371-375.
- Hayashida M, Maekawa F, Chagi Y, et al. Combination of multicolor flow cytometry for circulating lymphoma cells and tests for the *RHOA*(G17V) and *IDH2*(R172) hotspot mutations in plasma cell-free DNA as liquid biopsy for the diagnosis of angioimmunoblastic T-cell lymphoma. *Leuk Lymphoma*. 2020;61(10):2389-2398.
- Tanzima Nuhut S, Sakata-Yanagimoto M, Komori D, et al. Droplet digital polymerase chain reaction assay and peptide nucleic acid-locked nucleic acid clamp method for *RHOA* mutation detection in angioimmunoblastic T-cell lymphoma. *Cancer Sci*. 2018;109(5):1682-1689.
- Jaiswal S, Fontanillas P, Flannick J, et al. Age-related clonal hematopoiesis associated with adverse outcomes. *N Engl J Med*. 2014;371(26):2488-2498.
- Lewis NE, Petrova-Drus K, Huet S, et al. Clonal hematopoiesis in angioimmunoblastic T-cell lymphoma with divergent evolution to myeloid neoplasms. *Blood Adv*. 2020;4(10):2261-2271.
- Steciuk MR, Massengill S, Banks PM. In immunocompromised patients, Epstein-Barr virus lymphadenitis can mimic angioimmunoblastic T-cell lymphoma morphologically, immunophenotypically, and genetically: a case report and review of the literature. *Hum Pathol*. 2012;43(1):127-133.
- Nicolae A, Pittaluga S, Venkataraman G, et al. Peripheral T-cell lymphomas of follicular T-helper cell derivation with Hodgkin/Reed-Sternberg cells of B-cell lineage: both EBV-positive and EBV-negative variants exist. *Am J Surg Pathol*. 2013;37(6):816-826.
- Laforga JB, Gasent JM, Vaquero M. Potential misdiagnosis of angioimmunoblastic T-cell lymphoma with Hodgkin's lymphoma: a case report. *Acta Cytol*. 2010;54(5 Suppl):840-844.
- Tan LH, Tan SY, Tang T, et al. Angioimmunoblastic T-cell lymphoma with hyperplastic germinal centres (pattern 1) shows superior survival to patterns 2 and 3: a meta-analysis of 56 cases. *Histopathology*. 2012;60(4):570-585.
- Sakata-Yanagimoto M, Nakamoto-Matsubara R, Komori D, et al. Detection of the circulating tumor DNAs in angioimmunoblastic T-cell lymphoma. *Ann Hematol*. 2017;96(9):1471-1475.

24. Nguyen TB, Sakata-Yanagimoto M, Fujisawa M, et al. Dasatinib Is an effective treatment for angioimmunoblastic T-cell lymphoma. *Cancer Res.* 2020;80(9):1875-1884.
25. Attygalle AD, Diss TC, Munson P, Isaacson PG, Du MQ, Dogan A. CD10 expression in extranodal dissemination of angioimmunoblastic T-cell lymphoma. *Am J Surg Pathol.* 2004;28(1):54-61.
26. Vallois D, Dobay MP, Morin RD, et al. Activating mutations in genes related to TCR signaling in angioimmunoblastic and other follicular helper T-cell-derived lymphomas. *Blood.* 2016;128(11):1490-1502.
27. Rohr J, Guo S, Huo J, et al. Recurrent activating mutations of CD28 in peripheral T-cell lymphomas. *Leukemia.* 2016;30(5):1062-1070.
28. Fujisawa M, Sakata-Yanagimoto M, Nishizawa S, et al. Activation of RHOA-VAV1 signaling in angioimmunoblastic T-cell lymphoma. *Leukemia.* 2018;32(3):694-702.
29. Couronné L, Bastard C, Bernard OA. TET2 and DNMT3A mutations in human T-cell lymphoma. *N Engl J Med.* 2012;366(1):95-96.
30. Quivoron C, Couronné L, Della Valle V, et al. TET2 inactivation results in pleiotropic hematopoietic abnormalities in mouse and is a recurrent event during human lymphomagenesis. *Cancer Cell.* 2011;20(1):25-38.
31. Schwartz FH, Cai Q, Fellmann E, et al. TET2 mutations in B cells of patients affected by angioimmunoblastic T-cell lymphoma. *J Pathol.* 2017;242(2):129-133.
32. Ch'ang HJ, Su IJ, Chen CL, et al. Angioimmunoblastic lymphadenopathy with dysproteinemia--lack of a prognostic value of clear cell morphology. *Oncology.* 1997;54(3):193-198.